Tree Physiology Advance Access published October 21, 2013

Tree Physiology 00, 1–10
doi:10.1093/treephys/tpt077

Research paper

Photosynthesis of *Quercus suber* is affected by atmospheric NH_3 generated by multifunctional agrosystems

Marta Pintó-Marijuan[1,2,6], Anabela Bernardes Da Silva[3], Jaume Flexas[4], Teresa Dias[5], Olfa Zarrouk[1], Maria Amélia Martins-Loução[5], Maria Manuela Chaves[1] and Cristina Cruz[5]

[1]Molecular Ecophysiology Lab. (LEM), Instituto de Tecnologia Química e Biológica, Universidade Nova de Lisboa, 2780-901 Oeiras, Portugal; [2]Facultat de Biologia, Departament de Biologia Vegetal, Universitat de Barcelona, Av. Diagonal 643, E-08028 Barcelona, Spain; [3]Faculdade de Ciências, Centro para a Biodiversidade e Genómica Integrativa e Funcional (BioFIG), Universidade de Lisboa, Campo Grande, 1749-016 Lisboa, Portugal; [4]Grup de Recerca en Biologia de les Plantes en Condicions Mediterrànies, Departament de Biologia, Universitat de les Illes Balears, Carretera de Valldemossa Km 7.5, E-07122 Palma de Mallorca, Spain; [5]Faculdade de Ciências, Centro de Biologia Ambiental (CBA), Universidade de Lisboa, Campo Grande, 1749-016 Lisboa, Portugal; [6]Corresponding author (marta.pinto.marijuan@gmail.com)

Received June 6, 2013; accepted August 15, 2013; handling Editor Jörg-Peter Schnitzler

Montados are evergreen oak woodlands dominated by *Quercus* species, which are considered to be key to biodiversity conservation and ecosystem services. This ecosystem is often used for cattle breeding in most regions of the Iberian Peninsula, which causes plants to receive extra nitrogen as ammonia (NH_3) through the atmosphere. The effect of this atmospheric NH_3 (NH_{3atm}) on ecosystems is still under discussion. This study aimed to evaluate the effects of an NH_{3atm} concentration gradient downwind of a cattle barn in a Montado area. Leaves from the selected *Quercus suber* L. trees along the gradient showed a clear influence of the NH_3 on $\delta^{13}C$, as a consequence of a strong limitation on the photosynthetic machinery by a reduction of both stomatal and mesophyll conductance. A detailed study of the impact of NH_{3atm} on the photosynthetic performance of *Q. suber* trees is presented, and new mechanisms by which NH_3 affects photosynthesis at the leaf level are suggested.

Keywords: carbon isotopic discrimination, cork oak, mesophyll conductance, stomatal conductance.

Introduction

As the human population continues to expand, so does the global nitrogen (N) load on the biosphere as a result of increased agricultural activities and fossil fuel emissions, which have nearly doubled since the pre-industrial era (Erisman et al. 2008, Galloway et al. 2008, Rockstrom et al. 2009, Erisman et al. 2010). This relatively recent input of reactive N (all N forms except di-nitrogen, N_2) has a myriad of effects on water, soils, atmosphere and biosphere (Rockstrom et al. 2009). The overall environmental cost of all reactive N loads on the biosphere in Europe has been estimated to be €70–€320 billion per year, outweighing the direct economic benefits to agriculture of the application of reactive N as fertilizer (Sutton et al. 2011). For this reason, besides its scientific importance, the N issue has, at least in Europe, recently gained social, economic and political significance.

On the other hand, managed oak woodlands (Montados, dehesas) dominated by evergreen *Quercus* species, which are often used for cattle breeding in most regions of the Iberian Peninsula, represent a multifunctional integrated agro-silvo-pastoral system. High-quality pastures and agricultural cultivation areas coexist in the same spatial range, providing a good example of a 'human shaped' ecosystem (Bugalho et al. 2011). Consequently, vegetation receives an extra input of N through the atmosphere or the soil (farmyard manure), with likely impacts on plant productivity.

One major implication of the large increase in the reactive N gases delivered to the atmosphere each year is the deposition of this reactive N on the earth's surface. Current total ammonia (NH_3) emissions to the atmosphere are estimated to be 57 Tg N $year^{-1}$, with the largest contribution coming from

volatilization of animal wastes, 23 Tg N $year^{-1}$ (Erisman 2012). Both are increasing with time and are expected to be 50% larger by 2050 (Galloway et al. 2004). As atmospheric NH_3 (NH_{3atm}) readily deposits on any surface after emission (Krupa 2003), a large proportion of all emissions are intercepted by plant canopies. Leaf NH_3 uptake may occur though stomata and/or cuticle diffusion (Fernandez and Eichert 2009, Sparks 2009), depending on the relative NH_3 concentrations in the leaf apoplast and the atmosphere. However, actual NH_3 concentrations are dependent on the variables that determine the equilibrium between NH_3 and ammonium (NH_4^+), mainly water content and pH (Massad et al. 2010).

Several downstream molecular events derived from NH_3 deposition and nutrition have been described as related to C metabolism and energy, e.g., photosynthesis, ion balance, carbohydrate content, respiration rates, the futile cycle of NH_4^+ influx/efflux (Britto et al. 2001, Ariz et al. 2010, 2011, Balkos et al. 2010, Eichelmann et al. 2011), N primary metabolism (Cruz et al. 2006, 2011) and phytohormone and signalling molecules (Barth et al. 2010). When NH_3 enters the cells, it can rapidly be converted into NH_4^+, affecting all cell metabolism (Cruz et al. 2011). Ammonia/ammonium toxicity was explained either by the uncoupling of photophosphorylation, although not proven for whole organisms (Zhu et al. 2001, Britto and Kronzucker 2002), or as being an inhibitor of photosynthetic oxygen evolution (Sandusky and Yocum 1984). Recently, Polander and Barry (2012) indicated that a water-based hydrogen-bonding network plays a catalytic role in photosynthetic oxygen evolution, and that NH_3 or NH_4^+ may perturb or disrupt this network, due to the associated increase in bond strength. However, an overall view of the primary steps of NH_4^+ toxicity in relation to carbon (C) and N metabolism is still lacking, making it difficult to understand plants' physiological responses to NH_3.

We focused on four steps of photosynthetic mechanisms: (i) CO_2 conductance; (ii) leaf structure; (iii) chlorophyll composition and photosystem efficiency; and (iv) enzyme activity. The first step takes into account all the ways that CO_2 reaches chloroplasts and is assimilated by ribulose-1,5-bisphosphate carboxylase oxygenase (Rubisco). Boundary layers, stomata and mesophyll resistance are the main physical interferences to CO_2 assimilation (Flexas et al. 2008). Leaf structure also influences photosynthetic mechanisms: a thicker structure is very often correlated with a higher leaf mass per area (LMA) (Kogami et al. 2001, Poorter et al. 2009) and Hassiotou et al. (2010) positively correlated LMA and mesophyll cell wall thickness ($R^2 = 0.84$; $P_{value} = 0.01$), which clearly reduces the mesophyll conductance (Flexas et al. 2008, Tosens et al. 2012*b*). Finally, photosystem efficiency and the highest Rubisco activity affect photosynthesis promoting higher CO_2 assimilation rates (Adams et al. 2013, Parry et al. 2013).

The effect of the NH_3 load on ecosystems is still under discussion. This study examines the effect of a range of NH_{3atm} concentrations on the photosynthetic performance of a natural forest of *Quercus suber* L., opening up several hypotheses to understand the effects of high concentrations of NH_{3atm} on photosynthesis by woody plants.

Materials and methods

Experimental site

The study site is a cork oak (*Q. suber*) woodland (Montado) in the vicinity of an intensive livestock farm in Portugal (38.744583°N, 8.785405°W). The area has a Mediterranean climate (Rivas-Martínez et al. 2004): dry hot summers, mild rainy winters, average annual atmospheric temperature 17.5 °C and average annual precipitation 600 mm. Meteorological data were collected from the nearest station (38.724293°N, 9.011654°W), at the BA6 base of the Portuguese Air Force. The site does not suffer water limitation due to the presence of groundwater, 1 m below the soil surface. Intensive agricultural and livestock activities take place in the surroundings of the farm, and ~200 beef cows are permanently housed in a single barn measuring 800 m^2 (resulting in 24 kg N day^{-1} of extra N input). The soil at the site is sandy alluvial with wind deposits. Up to ~20 m from the barn, animals and machines continually disturb the soil by revolving it, while in the cork oak woodland, soil mobilization is minimal.

Atmospheric ammonia concentrations

Sampling locations (20) were chosen from 2 to 252 m along a transect downwind from the cattle barn. Atmospheric NH_3 concentrations at each location were measured using high-sensitivity adapted low-cost passive high absorption (ALPHA) passive diffusion samplers (Tang et al. 2001), placed 2 m above the ground. Ammonium concentrations on the filter papers collected in the ALPHA samplers (two samplers at each point) were determined by a modification of the Berthelot reaction (Cruz and Martins-Loução 2000; Pinho et al. 2012). Controls and calibrations of the quantification were performed as described in Pinho et al. (2012). Most sampling points were located within 200 m of the barn, where the atmospheric NH_3 gradient was expected to be highest (Sutton et al. 1998). [NH_{3atm}] values are the mean of monthly measurements taken during 1 year, expressed in µg m^{-3}.

Leaf sampling

From each *Q. suber*, tree leaves were collected and pooled. Pools were composed of at least 25 current-year, fully expanded, sun-exposed (south orientation). Leaves were detached in the middle of the day, immediately frozen in N_2 liquid and stored at –80 °C until biochemical analyses. Two leaf samplings (LSs) were performed: LS1 and LS2. Trees were selected randomly along the transect from the barn to 250 m away. In LS1, 20 different cork oak trees were selected and in LS2 eight to nine trees.

Leaf NH_4^+ concentration

Each pool of leaves from LS1 was washed with deionised water three times for 30 s, and the water was discarded. Ammonium was determined in extracts prepared by grinding the leaves with liquid N, then adding distilled water at a ratio of 1 g fresh weight:10 ml. Extracts were centrifuged at 5000*g* at 4 °C and the absorbance of the supernatant was measured as described in the 'Atmospheric ammonia concentrations' section.

Leaf stable C isotope ratios

Five to eight milligrams of powdered plant material from each sample collected in LS1 were separately packed in tin capsules and $^{13}C/^{12}C$ isotope ratios were determined by isotope ratio mass spectrometry (IsoPrime Isotope Ratio Mass Spectrometer, Micromass-GV Instruments, Cheadle Hulme, UK) as described in Werner et al. (2006). The leaf C isotope ratio was expressed in delta notation as:

$$\delta^{13}C_{sample}(‰) = \left(\frac{R_{sample}}{R_{standard}} - 1\right) \times 1000$$

where $\delta^{13}C_{sample}$ is the isotope ratio in parts per thousand (‰), R_{sample} and $R_{standard}$ are the $^{13}C/^{12}C$ molar abundance ratios of the leaf material and the Pee Dee Belemnite standard. Isotope ratios were calibrated against international standards: IAEA CH6 (sucrose) and IAEA CH7 (polyethylene) for C isotope ratios and IAEA N1 (ammonium sulfate) for N isotope ratios (Rodrigues et al. 2011).

Relative water content determination and leaf morphology

On eight trees selected for LS2, the relative water content (%RWC) of leaves and the LMA were measured. The %RWC was obtained from the formula: (FW – DW)/(FSW – DW) × 100, where FW is the fresh weight, FSW is the fresh saturated weight after rehydrating samples for 24 h in the dark at 4 °C and DW is the dry weight after oven-drying samples at 65 °C until constant weight. The leaf area (LA) was measured with a flat-bed scanner (Epson Perfection V30) and processed using the LA Measurement program (Version 1.3, The University of Sheffield, 2003) image analyzer software. The LMA was calculated as DW/LA. Values given are the means of three independent samples per tree (with four leaves per sample).

Gas exchange and chlorophyll fluorescence measurements

Leaf gas exchange measurements coupled to chlorophyll fluorescence were performed between 10:00 and 16:00 on two attached leaves of each of the nine trees selected for LS2, with a portable infrared gas analyzer (LI-6400 system, LI-COR, Inc., Lincoln, NE, USA) using a leaf chamber fluorometer. In order to determine the saturation light for C assimilation, the net CO_2 assimilation (A) response curves to photosynthetic photon flux density (PPFD) ($A/PPFD$) were determined. During the measurements, leaves were maintained at 20 °C, and the supplied CO_2 concentration inside the cuvette (C_a) was 400 μmol mol^{-1} CO_2. Light intensity during $A/PPFD$ measurements decreased from 2000 to 0 μmol m^{-2} s^{-1} as follows: 2000, 1500, 1000, 750, 500, 250, 100, 50 and 0 μmol m^{-2} s^{-1}. Dark respiration (R_n) was measured in dark-adapted leaves on four trees. Under these conditions, *Q. suber* trees showed light-saturated photosynthesis at 1500 μmol m^{-2} s^{-1}. As a consequence, to determine A/intercellular CO_2 concentration (C_i) response curves to the internal CO_2 concentration, the PPFD was maintained at 1500 μmol m^{-2} s^{-1} (with 10% blue light) and C_i started at 400 μmol mol^{-1}, decreasing stepwise to 200, 100 μmol mol^{-1} and then increasing from 100 stepwise to 150, 200, 250, 350, 500, 750, 1000, 1200, 1500, 1750 μmol mol^{-1}. The leaf temperature was maintained at 20 °C.

Analyses of the measured A/C_i curves allowed the determination of net CO_2 assimilation at saturating C_i (A_{max}). The maximum apparent carboxylation velocity (V_{c,max_Ci}) for the distinct leaves was determined by fitting a maximum likelihood regression below and above the inflexion of the A/C_i response, using K_c, K_o (Michaelis–Menten constants for CO_2 and O_2, respectively) as described by McMurtrie and Wang (1993). Values (C_a: 350 μmol mol^{-1}) of stomatal conductance (gs_{350}), CO_2 assimilation rate (A_{350}) and intrinsic water use efficiency ($WUE_{i\_350} = A_{350}/g_{s\_350}$) at CO_2 close to atmospheric concentration were also calculated.

Chlorophyll fluorescence was determined concomitantly with each gas exchange measurement. From the fluorescence measurements, the actual quantum efficiency of the photosystem II (PSII)-driven electron transport (Φ_{PSII}) was determined according to Genty et al. (1989), and the rate of linear electron transport (ETR) was calculated as described in Flexas et al. (2007). The maximum photochemical efficiency of PSII (F_v/F_m) was estimated using a portable fluorimeter (Mini-PAM; Walz, Effeltrich, Germany) in three to five dark-adapted (30 min) leaves in the same trees at midday, as described by Pinto-Marijuan et al. (2007).

Estimation of mesophyll conductance

From combined gas exchange and chlorophyll *a* fluorescence measurements, the mesophyll conductance for CO_2 (g_m) was estimated according to Harley et al. (1992) by assuming that the electron transport rates calculated by gas exchange and by fluorescence match in the absence of internal resistance and photorespiration (PR, Loreto et al. 1992). Calculated values of g_m were used to convert A/C_i curves to A/C_c curves according to the following equation:

$$C_c = C_i - \left(\frac{A}{g_m}\right)$$

Night respiration (R_n) was used in the experiments as a proxy for R_d by dividing R_n by 2 (Villar et al. 1995, Niinemets et al. 2005). The method of Farquhar et al. (1980) as described in Galle et al. (2011) was used for fitting A/C_c curves, from which g_m at ambient CO_2 concentration (g_{m_350}) was estimated and the maximum velocity of carboxylation by Rubisco (V_{c,max_Cc}) was calculated according to Bernacchi et al. (2002).

Rubisco activity and chloroplastic pigments quantification

Rubisco was extracted from *Q. suber* leaves from LS2. Enzyme extraction and determination of total activity (v_t) by the incorporation of $^{14}CO_2$ into acid-stable products at 25 °C in an O_2-free medium were carried out according to Carmo-Silva et al. (2010). Spectrophotometric measurements to quantify the chloroplastic pigments were performed according to Lichtenthaler (1987).

Statistical analysis

To evaluate the effect of N on the measured traits, the mean values obtained for each parameter on each *Q. suber* tree were compared by a linear regression analysis. R^2 and P_{values} were calculated using the SPSS 15.0 statistical package (SPSS, Inc., Chicago, IL, USA). They are represented in the text and figures as follows: $P \leq 0.01$ (***); $0.01 < P \leq 0.05$ (**); $0.05 < P \leq 0.1$ (*). Statistical graphs were prepared using SigmaPlot 10.0 (Systat Software, Inc., San Jose, CA, USA).

Results

Leaf NH_4^+ concentrations increased according to the distance from the barn

Atmospheric ammonia concentrations were the highest (>30 μg m^{-3}), close to the cattle barn (Figure 1a), but dropped markedly along the first 50 m of the transect to <10 μg m^{-3}, stabilizing to background values (<5 μg m^{-3}) beyond 150 m from the barn. Figure 1b shows a good correlation between $[NH_4]_{leaf}$ and distance from the barn, suggesting that the NH_{3atm} from the barn was able to penetrate leaf tissues.

^{13}C Discrimination along the NH_{3atm} gradient

Leaves from trees near the barn were more enriched in ^{13}C (less negative $\delta^{13}C$ values) than those sampled further from the barn (Figure 1c). The lowest discrimination values were found in the leaves with the highest $[NH_4]_{leaf}$ (Figure 1c, inset; $R^2 = 0.802$***), indicating that NH_{3atm} was able to penetrate the leaf tissues and alter their physiological processes. The parameters NH_{3atm}, $[NH_4]_{leaf}$ and $\delta^{13}C$ were not linearly correlated with the distance from the barn, all decreased exponentially. On the other hand, $\delta^{13}C$ was linearly and positively correlated with $[NH_4]_{leaf}$. When both parameters were compared with photosynthetic characterization, $\delta^{13}C$ always gave the best correlations. This high correlation between $\delta^{13}C$ and NH_{3atm} thus allowed the use of $\delta^{13}C$ as an indicator of the prevailing NH_{3atm} surrounding other sampled trees.

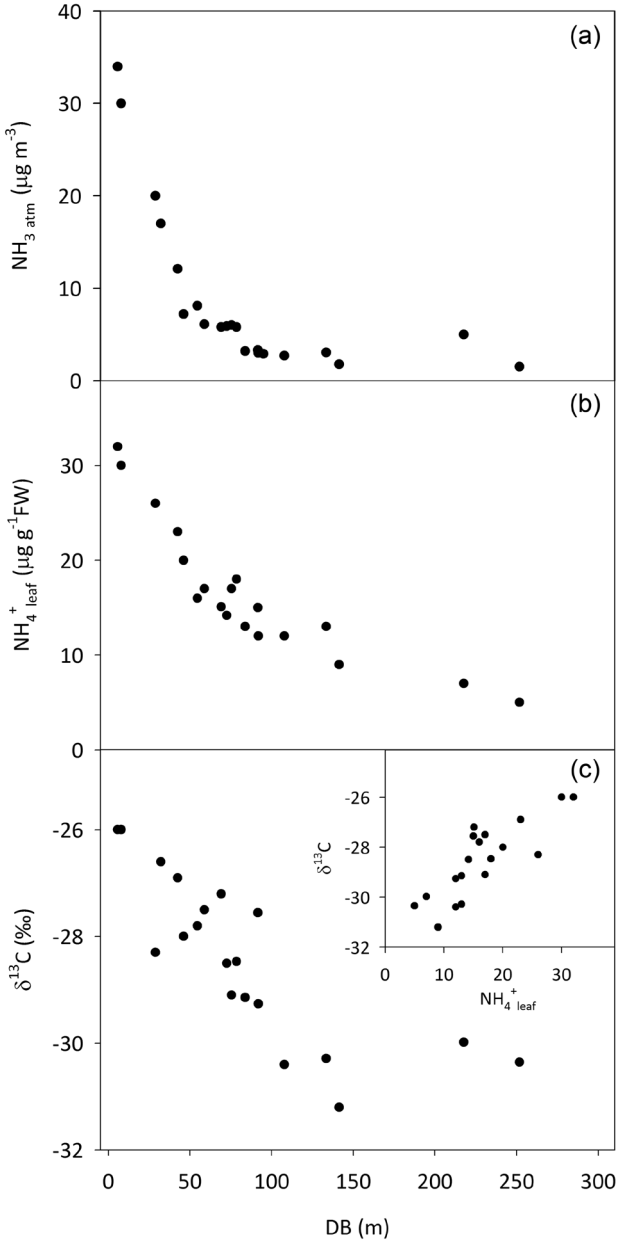

Figure 1. Characterization of the surrounding community along the transect, in relation to the distance from the barn (DB): (a) atmospheric ammonia profile (NH_{3atm} in μg m^{-3}); (b) ammonium concentration ($[NH_4]_{leaf}$ in μg g^{-1} FW) in *Q. suber* leaves; and (c) isotopic composition of ^{13}C ($\delta^{13}C$ in ‰) in the same leaves. Inset graph correlates $[NH_4]_{leaf}$ with $\delta^{13}C$ in the sampled leaves.

Two structural parameters were characterized at leaf level (Figure 2): thickness (via LMA) and water content (%RWC). No relation was found between leaf isotopic composition and LMA (Figure 2a; $R^2 = 0.168$). Leaf %RWC was significantly and positively correlated with $\delta^{13}C$ along the transect (Figure 2b; $R^2 = 0.824$***).

Photosynthetic characterization

Assimilation response curves to the internal CO_2 concentration (A/C_i) were determined to identify any effects on physiological

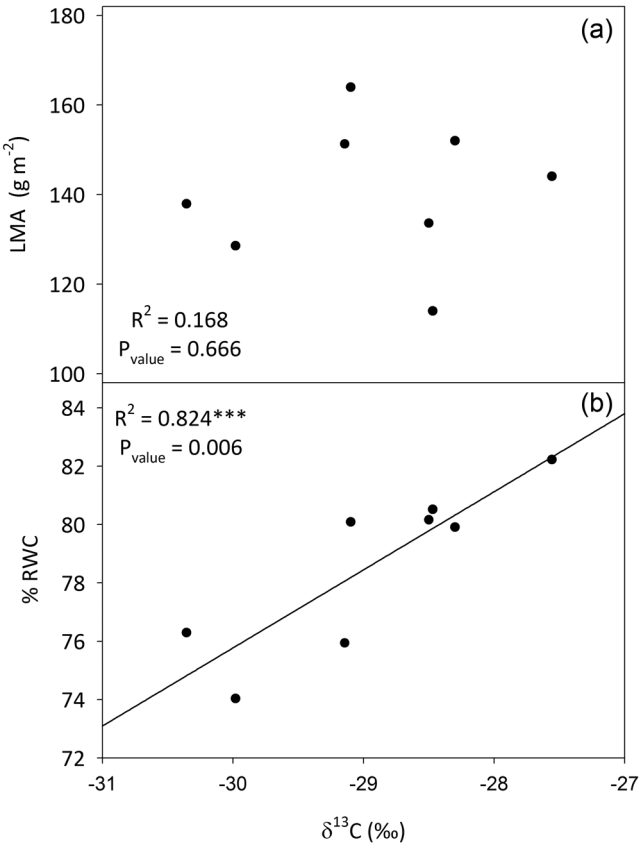

Figure 2. Relationships between leaf isotopic composition (δ^{13}C, ‰) and physical characteristics of *Q. suber* leaves: (a) leaf thickness expressed as LMA (g DW m^{-2}); and (b) %RWC. The regression coefficients and significance of each relationship are shown in each graph. Asterisks represent the significance as follows: $P_{value} \leq 0.01$ (***), $0.01 < P_{value} \leq 0.05$ (**), $0.05 < P_{value} \leq 0.1$ (*).

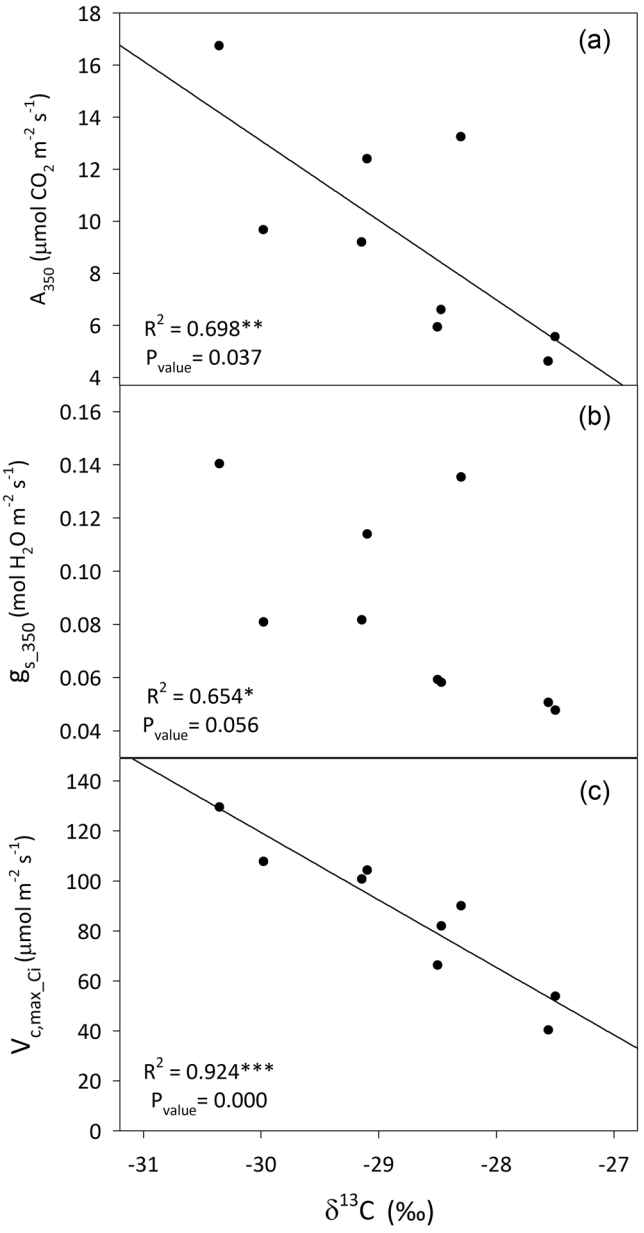

Figure 3. Photosynthetic parameters (calculated from the A/C_i response curves) as a function of isotopic composition (δ^{13}C, ‰) of *Q. suber* leaves: (a) Net CO_2 assimilation at ambient CO_2 (A_{350} in µmol CO_2 m^{-2} s^{-1}); (b) stomatal conductance at ambient CO_2 (g_{s_350} in mol H_2O m^{-2} s^{-1}); and (c) maximum apparent carboxylation velocity ($V_{c,max}$ in µmol m^{-2} s^{-1}). The regression coefficients and significance of each relationship are shown in each graph. Asterisks represent the significance as follows: $P_{value} \leq 0.01$ (***), $0.01 < P_{value} \leq 0.05$ (**), $0.05 < P_{value} \leq 0.1$ (*).

mechanisms. Net CO_2 assimilation rate (A_{350}; Figure 3a: $R^2 = 0.698$**) and stomatal conductance (g_{s_350}; Figure 3b: $R^2 = 0.654$*) were negatively correlated with the δ^{13}C. The strongest negative correlation with ^{13}C discrimination was found with the maximum carboxylation velocity of Rubisco ($V_{c,max}$; Figure 3c: $R^2 = 0.924$***). This correlation showed a sharp fall in V_{c,max_Ci} from 140 to 40 µmol m^{-2} s^{-1} along the NH_{3atm} gradient. $[NH_4]_{leaf}$ affected gas exchange parameters in the studied *Q. suber* trees, reducing the net CO_2 fixation (A_{350}) by reducing both g_{s_350} and apparent V_{c,max_Ci}.

Some of the factors expected to affect V_{c,max_Ci} were as follows: (i) chlorophyll content (Chl *a* + Chl *b*; Figure 4a); (ii) total Rubisco activity expressed per Chl unit (v_t; Figure 4b); and (iii) photoinhibition, represented by the maximum quantum yield of PSII measured after PSII relaxation in the dark (F_v/F_m; Figure 4c). However, none of these showed any significant correlation with the C isotopic composition, indicating that they had no effect on V_{c,max_Ci}.

Another factor expected to lower V_{c,max_Ci} was a decreased mesophyll conductance to CO_2, which would result in a much lower CO_2 chloroplast concentration (C_{c_350}) than C_i. A good correlation between C_{c_350} and δ^{13}C was indeed observed (Figure 5a; $R^2 = 0.555$). The C_{c_350} data allowed the recalculation of the maximum velocity of carboxylation by Rubisco based on the chloroplast concentration of CO_2 (Figure 5b; V_{c,max_Cc}). These calculations showed that there were no significant differences between the carboxylation velocities of the studied *Q. suber* trees when the C_{c_350} values at the real Rubisco site were taken into account. C_{c_350} values also allowed the calculation of the mesophyll

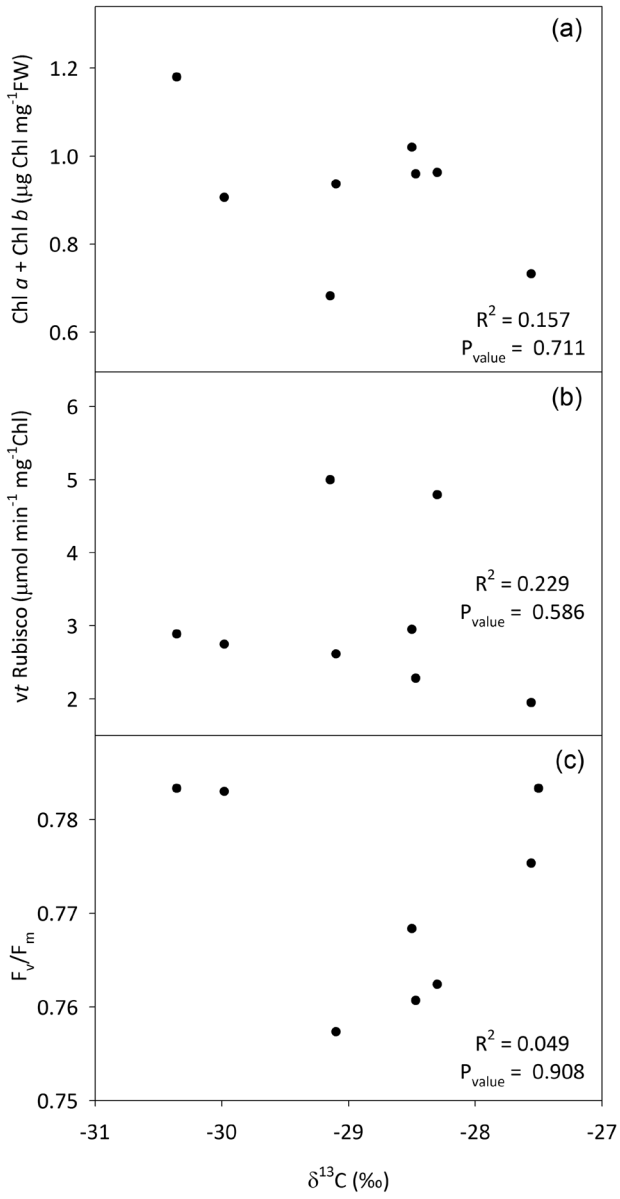

Figure 4. Photosynthetic parameters of *Q. suber* leaves as a function of the leaf isotopic composition ($\delta^{13}C$, ‰): (a) Total chlorophyll content in µg of pigment mg^{-1} FW; (b) total Rubisco activity (v_t) in µmol of enzyme per min expressed per milligram of total chlorophyll; and (c) maximum photochemical efficiency of PSII (F_v/F_m). The regression coefficients and significance of each relationship are shown in each graph. Asterisks represent the significance as follows: $P_{value} \leq 0.01$ (***), $0.01 < P_{value} \leq 0.05$ (**), $0.05 < P_{value} \leq 0.1$ (*).

conductance at the ambient CO_2 concentration (g_{m_350}; Figure 5c). g_{m_350} was highly correlated with $\delta^{13}C$ ($R^2 = 0.748$**). The ratios of PR to assimilation calculated at ambient CO_2 concentration (Figure 5d; PR_{350}/A_{350}) showed that the highest PR ($R^2 = 0.647$*) occurred in trees grown under the highest $[NH_{3atm}]$.

Discussion

Montados are traditionally used for free-range cattle breeding, but the application of intensive farming, whereby cattle are raised in barns at high densities for part of their lives, is spreading. The Montado area studied in the present work is composed of a *Q. suber* forest where an intensive cattle barn was installed, giving rise to a point source of NH_{3atm} (Pinho et al. 2011) which generates a downwind decreasing gradient of $[NH_{3atm}]$. The movement of NH_3 through the atmosphere is highly dependent on the wind speed, humidity and temperature (Krupa 2003). Since it readily settles on any surface after emission, plant canopies are prone to large deposits of this pollutant (Krupa 2003). In fact, the similarity between observed patterns of $[NH_{3atm}]$ and $[NH_4]_{leaf}$ along the transect from the barn showed that the cork oak canopies were intercepting $[NH_{3atm}]$. After deposition on a leaf's surface, NH_3 may be taken up through stomata and/or cuticle diffusion (Fernandez and Eichert 2009, Sparks 2009), so leaf uptake of gaseous NH_3 by *Q. suber* was expected to be strongly related to stomatal conductance (Gessler et al. 2000, 2002). Our study showed a negative effect of $[NH_{3atm}]$ on the stomatal aperture (Figure 3b). The different slopes in Figure 1a (higher slope in $[NH_{3atm}]$) and Figure 1b (softer slope of $[NH_4]_{leaf}$), due to greater closure of stomata under higher NH_{3atm} concentrations, reinforce the hypothesis that g_{s_350} affects the entrance of NH_{3atm} into the leaf. The diffusion of NH_3 into the leaf appoplast is driven by the concentration gradient between the NH_3 in the air of the sub-stomatal space and the surrounding mesophyll tissue (Krupa 2003). Moreover, the high $[NH_4]_{leaf}$ found in our experimental trees (>30 µg g^{-1} FW) revealed some capacity to store NH_4^+ (in the apoplast or in cellular vacuoles), as previously observed in studies conducted at very high NH_3 concentrations (Grundmann et al. 1993, Qiao and Murray 1997).

Leaf isotopic composition data showed that different photosynthetic processes were occurring along the gradient. During photosynthetic CO_2 fixation, fractionation of stable C isotopes occurs and plants consequently become generally depleted in the heavier isotope ^{13}C (Brugnoli and Farquhar 2004). The major steps that discriminate against the heaviest molecule of CO_2 ($^{13}CO_2$) are biochemical discrimination by the carboxylating enzyme, Rubisco (27–30‰), and the limitations of gaseous diffusive transport from the atmosphere to the carboxylation site (4.4‰) (Farquhar et al. 1982, 1989). Our data showed lower CO_2 discrimination processes at high NH_{3atm} concentrations, indicating that it was difficult for CO_2 molecules to reach the chloroplasts on the leaves of the trees that were more exposed to the barn atmosphere. Moreover, our study found CO_2 assimilation (A_{350}) to be strongly correlated with $\delta^{13}C$ in *Quercus* trees, indicating that the NH_{3atm} gradient negatively affected CO_2 fixation. Leaves of trees closer to the barn had lower A_{350}, g_{s_350} and very low V_{c,max_Ci} values (Figure 3); lower stomatal conductance interferes with the movement of CO_2 molecules to the mesophyll, reducing CO_2 availability at Rubisco sites and, therefore, reducing enzymatic discrimination and apparent $V_{c,max}$. g_{s_350} also interferes with the movement of H_2O

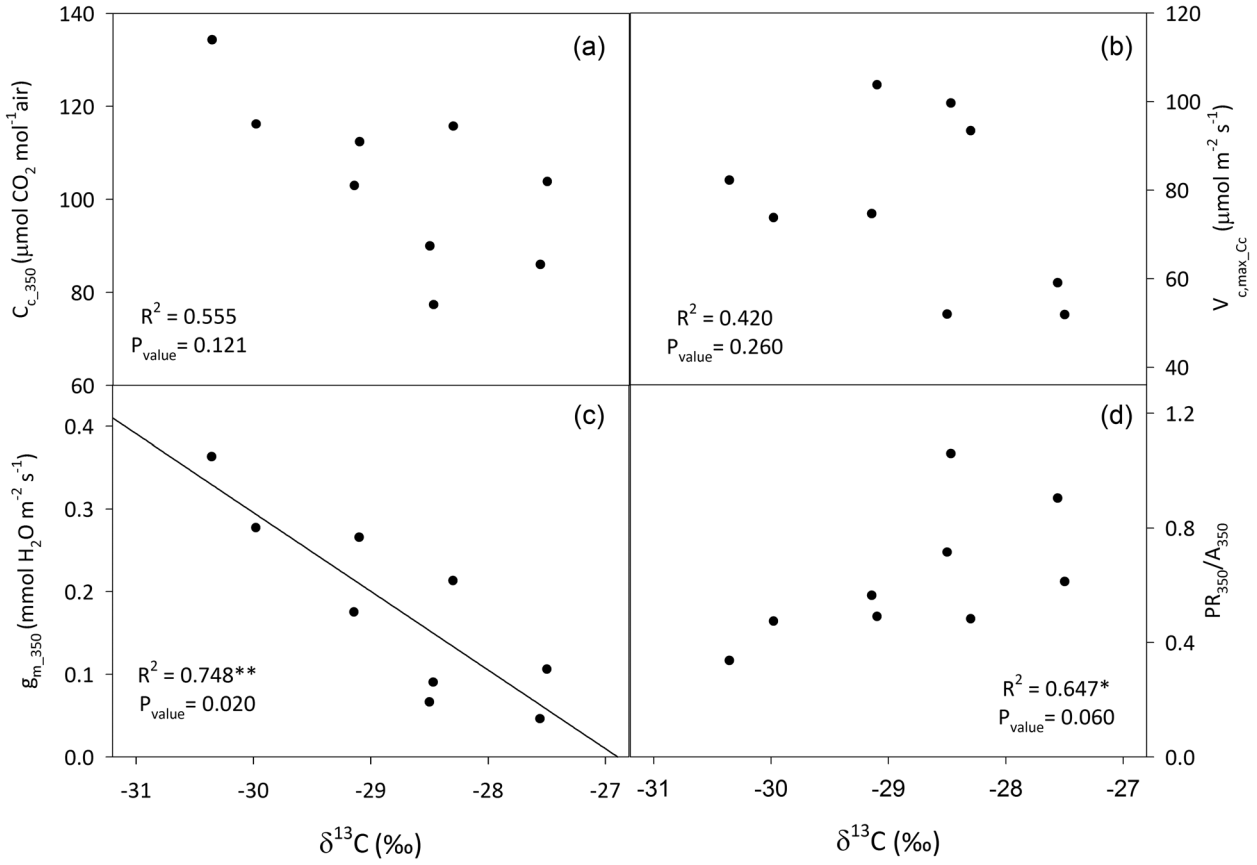

Figure 5. Photosynthetic parameters calculated from A/C_c response curves as a function of isotopic composition ($\delta^{13}C$, ‰) of *Q. suber* leaves: (a) CO_2 concentration in the chloroplast at ambient CO_2 (C_c in µmol CO_2 mol^{-1}air); (b) maximum apparent carboxylation velocity (V_{c,max_Cc} in µmol m^{-2} s^{-1}); (c) mesophyll conductance at ambient CO_2 (g_{m_350} in mmol H_2O m^{-2} s^{-1}); and (d) PR divided by net CO_2 assimilation at ambient CO_2 (PR_{350}/A_{350}). The regression coefficients and significance of each relationship are shown in each graph. Asterisks represent the significance as follows: $P_{value} \leq 0.01$ (***), $0.01 < P_{value} \leq 0.05$ (**), $0.05 < P_{value} \leq 0.1$ (*).

molecules from the mesophyll to the atmosphere. Given that water was not a limiting factor on the studied area, we suggest that the strong correlation between $\delta^{13}C$ and leaf %RWC (Figure 2b) observed among the *Q. suber* trees supported lower stomatal aperture on the trees closer to the barn. In addition, the PR/*A* ratio at ambient CO_2 concentration (PR_{350}/A_{350}; Figure 5d) showed that the trees with the highest PR ($R^2 = 0.608$*) grew under the highest [NH_3]. Our results are in concordance with the findings of Lanigan et al. (2008), who tested the discrimination of glycine decarboxylase against ^{13}C, and concluded that the higher PR implied enriched tissues. Moreover, high PR decreases the apparent conductance of CO_2 diffusion to the chloroplast (Tholen and Zhu 2011). These parameters coherently indicate a photosynthetic limitation on the trees near the barn, a limitation which may be mediated by $[NH_4]_{leaf}$.

Several factors that have been previously been indicated to be influenced by [NH_3] (Ariz et al. 2010, Pompelli et al. 2010) could be the cause of this constraint: lower chlorophyll content, Rubisco concentration or photoinhibition. Chlorophyll content was observed to increase with higher [NH_3], but data from our experimental site trees (Chl *a* + Chl *b* in Figure 4a) did not reveal any significant correlation between chlorophylls and C isotopic discrimination, and therefore NH_{3atm}. The Rubisco content has previously been observed to be higher at high concentrations of NH_4^+ in the growing media (Ariz et al. 2010); however, this study did not find any correlation between variations in v_t (Figure 4b) and NH_{3atm}. Finally, the maximum quantum yield of PSII photochemistry measured after PSII relaxation in the dark (F_v/F_m; Figure 4c) might have been affected by [NH_3] also reducing photosynthetic capacity in high-NH_3 growing plants; however, no such effect was detected along the gradient.

Isotopic discrimination is also related to structural leaf parameters, which can interfere with CO_2 diffusion, such as LMA, an integrative measurement of thickness and density (Fleck et al. 2010). Thickness can limit the ability of CO_2 molecules to reach the chloroplast (Tosens et al. 2012*b*), contributing to the reduction of discrimination at the Rubisco level. However, our study did not reveal any differences in LMA along the NH_3 gradient, indicating that it was not limited by thicker mesophyll cell walls along the gradient. V_{c,max_Ci} was not a good proxy for Rubisco activity (Figure 3c) when g_m was ignored, as

already demonstrated in several publications (Flexas et al. 2007, 2012). No correlation was found between isotopic composition along the NH_3 gradient and V_{c,max_Cc} (Figure 5b). These data indicate that Rubisco activity in leaves was stable along the NH_{3atm} gradient (Figure 4b). However, a clear and strong correlation ($R^2 = 0.856$; $P = 0.003$) was found between mesophyll conductance for CO_2 (g_m) at ambient CO_2 concentration (Figure 5c; g_{m_350}) and $\delta^{13}C$, indicating that the trees closer to the barn, which had higher concentrations of NH_4^+ in their leaves, presented a high resistance to movement of CO_2 through the mesophyll to the chloroplast lumen.

This is the first time that g_m has been found to be affected by leaf and NH_{3atm} concentrations. Here, we present two hypothetical mechanisms of how NH_3 may interfere with C_{c_350} and g_m: (i) anatomical characteristics and (ii) differing aquaporin composition.

First, mesophyll conductance is directly correlated with distinct sclerophyll anatomical characteristics (Tosens et al. 2012*b*). The strongest sources of g_m variation are the exposed surface area of chloroplasts per unit LA (S_c/S) and the mesophyll cell wall thickness (t_{cw}). Since our study did not observe any changes in LMA, it is not likely that large changes in t_{cw} occurred, which leaves us with the hypotheses that chloroplast structure alters as a function of $[NH_4]_{leaf}$. Differences at the chloroplast level have been found in *Moricandia arvensis* grown under an NH_3 source (Winter et al. 1982), and in *Pinus sylvestris* subjected to NH_3 deposition in a fur farm (Back et al. 1997). Structural rearrangements are directly correlated with changes in the g_m data (Tosens et al. 2012*a*), so we hypothesize that NH_3 could be increasing mesophyll limitations.

Second, aquaporins (AQPs) are water-transporting membrane channel proteins that have also been described as gas channels (Maurel et al. 2008, Herrera and Garvin 2011) ruling CO_2 uptake in both *Nicotiana* and *Arabidopsis* (Uehlein et al. 2008, 2012). Other studies (Kaldenhoff et al. 2008; Flexas et al. 2012) have already described how AQPs facilitate CO_2 mesophyll conductance. It is now known that some AQPs can also transport NH_3 and are widely distributed in cell organelles (Tyerman et al. 2002; Kruse et al. 2006; Hove and Bhave 2011). Musa-Aziz et al. (2009) described animal/human AQP1 as the only AQP able to transport both CO_2 and NH_3, while Wudick et al. (2009) suggested that in plants *At*TIP1;1 and *At*TIP2;1 are located in the chloroplast and are responsible for NH_3 transport, as described by Ferro et al. (2003). The latter authors also mentioned the possible role of AQP in turgor of stomatal guard cells, as previously suggested by MacRobbie (2006). In summary, we hypothesize that a competition at the chloroplast level between CO_2 and NH_3 may occur as a result of: (i) competition inside of the organelle for the same AQP and/or (ii) higher concentrations of NH_3 could induce a greater expression of NH_3 AQP transporters than CO_2 AQP transporters. Whatever the exact mechanisms, a reduced mesophyll conductance at the highest $[NH_{3atm}]$ sites occurs, resulting in a restriction of CO_2 availability at the Rubisco inside the chloroplast, leading to reduced photosynthesis in oak trees.

Conclusions

Atmospheric ammonia is considered to be an air pollutant. Our results indicate that high levels of $[NH_{3atm}]$ inhibit the photosynthetic activity of *Q. suber* leaves. This inhibition may be explained by the lower stomatal conductance to CO_2 and the highest resistance of the leaf mesophyll to CO_2 movement, which decreases the availability of CO_2 for carboxylation by Rubisco. This is of particular importance since mesophyll conductance, one of the parameters shown to be affected by $[NH_{3atm}]$, is not considered in the majority of models of photosynthetic responses to environmental changes. Although the mechanisms of interaction between NH_3 and CO_2 are still far from understanding, this study opens the prospect of investigating the mechanisms by which NH_3 affects photosynthesis at the leaf level, then scaling this understanding up to models of communities and ecosystems. In consequence, we conclude this study with the prediction that if Montado management continues to allow the inclusion of cattle barns, these should be designed taking into account the effect of high NH_3 concentrations on cork oak productivity. The negative effects of high NH_4^+ concentrations on the receptor ecosystem could be, at least partially, mitigated by creating tree barriers around animal barns.

Acknowledgments

We thank Catarina Martins and Dr Marjan Jongen for assistance during the field sampling and Steve Houghton for English revision of the manuscript.

Conflict of interest

None declared.

Funding

M.P.-M. is supported by a fellowship granted by Generalitat de Catalunya (BP-A 00261). The Portuguese Foundation for Science and Technology (FCT) project PTDC/BIA-BEC/099323/2008 provided funds to support the research. J.F. acknowledges funding from Spanish Ministry of Science and Innovation Project BFU2011-23294 (MECOME).

References

Adams WW III, Muller O, Cohu CM, Demmig-Adams B (2013) May photoinhibition be a consequence, rather than a cause, of limited plant productivity? Photosynth Res doi:10.1007/s11120-013-9849-7.

Ariz I, Esteban R, Garcia-Plazaola JI, Becerril JM, Aparicio-Tejo PM, Moran JF (2010) High irradiance induces photoprotective mechanisms and a positive effect on NH_4^+ stress in *Pisum sativum* L. J Plant Physiol 167:1038–1045.

Ariz I, Artola E, Cabrera Asensio A, Cruchaga S, Maria Aparicio-Tejo P, Fernando Moran J (2011) High irradiance increases NH_4^+ tolerance in *Pisum sativum*: higher carbon and energy availability improve ion balance but not N assimilation. J Plant Physiol 168:1009–1015.

Back J, Turunen M, Ferm A, Huttunen S (1997) Needle structures and epiphytic microflora of Scots pine (*Pinus sylvestris* L.) under heavy ammonia deposition from fur farming. Water Air Soil Poll 100:119–132.

Balkos KD, Britto DT, Kronzucker HJ (2010) Optimization of ammonium acquisition and metabolism by potassium in rice (*Oryza sativa* L. cv. IR-72). Plant Cell Environ 33:23–34.

Barth C, Gouzd ZA, Steele HP, Imperio RM (2010) A mutation in GDP-mannose pyrophosphorylase causes conditional hypersensitivity to ammonium, resulting in *Arabidopsis* root growth inhibition, altered ammonium metabolism, and hormone homeostasis. J Exp Bot 61:379–394.

Bernacchi CJ, Portis AR, Nakano H, von Caemmerer S, Long SP (2002) Temperature response of mesophyll conductance. Implications for the determination of Rubisco enzyme kinetics and for limitations to photosynthesis in vivo. Plant Physiol 130:1992–1998.

Britto DT, Kronzucker HJ (2002) NH_4^+ toxicity in higher plants: a critical review. J Plant Physiol 159:567–584.

Britto DT, Siddiqi MY, Glass ADM, Kronzucker HJ (2001) Futile transmembrane NH_4^+ cycling: a cellular hypothesis to explain ammonium toxicity in plants. Proc Natl Acad Sci USA 98:4255–4258.

Brugnoli E, Farquhar G (2004) Photosynthetic fractionation of carbon isotopes. In: Leegood R, Sharkey T, Caemmerer S (eds) Photosynthesis. Springer, Netherlands, pp 399–434.

Bugalho MN, Caldeira MC, Pereira JS, Aronson J, Pausas JG (2011) Mediterranean cork oak savannas require human use to sustain biodiversity and ecosystem services. Front Ecol Environ 9:278–286.

Carmo-Silva AE, Keys AJ, Andralojc PJ, Powers SJ, Arrabaça MC, Parry MAJ (2010) Rubisco activities, properties, and regulation in three different C4 grasses under drought. J Exp Bot 61:2229–2234.

Cruz C, Martins-Loução MA (2000) Determination of ammonium concentrations in soils and plant extracts. In: Martins-Loução MA, Lips SH (eds) Nitrogen in a sustainable ecosystem: from the cell to the plant. Backhuys Publishers, Leiden, The Netherlands, pp 291–297.

Cruz C, Bio AFM, Dominguez-Valdivia MD, Aparicio-Tejo PM, Lamsfus C, Martins-Loucao MA (2006) How does glutamine synthetase activity determine plant tolerance to ammonium? Planta 223:1068–1080.

Cruz C, Domínguez-Valdivia MD, Aparicio-Tejo PM, Lamsfus C, Bio A, Martins-Loução MA, Moran JF (2011) Intra-specific variation in pea responses to ammonium nutrition leads to different degrees of tolerance. Environ Exp Bot 70:233–243.

Eichelmann H, Oja V, Peterson RB, Laisk A (2011) The rate of nitrite reduction in leaves as indicated by O_2 and CO_2 exchange during photosynthesis. J Exp Bot 62:2205–2215.

Erisman JW (2012) The European nitrogen problem in a global perspective. In: Sutton MA, Howard C, Erisman JW, Billen G, Bleeker A, Grenfelt P, van Grinsven H, Grizzetti B (eds) European nitrogen assessment. Cambridge Press, Cambridge, pp 68–79.

Erisman JW, Sutton MA, Galloway J, Klimont Z, Winiwarter W (2008) How a century of ammonia synthesis changed the world. Nat Geosci 1:636–639.

Erisman JW, van Grinsven H, Leip A, Mosier A, Bleeker A (2010) Nitrogen and biofuels: an overview of the current state of knowledge. Nutr Cycl Agroecosys 86:211–223.

Farquhar GD, Caemmerer SV, Berry JA (1980) A biochemical-model of photosynthetic CO_2 assimilation in leaves of C3 species. Planta 149:78–90.

Farquhar GD, Oleary MH, Berry JA (1982) On the relationship between carbon isotope discrimination and the intercellular carbon dioxide concentration in leaves. Aust J Plant Physiol 9:121–137.

Farquhar GD, Ehleringer JR, Hubick KT (1989) Carbon isotope discrimination and photosynthesis. Annu Rev Plant Physiol Plant Mol Biol 40:503–537.

Fernandez V, Eichert T (2009) Uptake of hydrophilic solutes through plant leaves: current state of knowledge and perspectives of foliar fertilization. Crit Rev Plant Sci 28:36–68.

Ferro M, Salvi D, Brugiere S, Miras S, Kowalski S, Louwagie M, Garin J, Joyard J, Rolland N (2003) Proteomics of the chloroplast envelope membranes from *Arabidopsis thaliana*. Mol Cell Proteomics 2: 325–345.

Fleck I, Pena-Rojas K, Aranda X (2010) Mesophyll conductance to CO_2 and leaf morphological characteristics under drought stress during *Quercus ilex* L. resprouting. Ann Forest Sci 67: Art. no. 308.

Flexas J, Ortuno MF, Ribas-Carbo M, Diaz-Espejo A, Florez-Sarasa ID, Medrano H (2007) Mesophyll conductance to CO_2 in *Arabidopsis thaliana*. New Phytol 175:501–511.

Flexas J, Ribas-Carbo M, Diaz-Espejo A, Galmes J, Medrano H (2008) Mesophyll conductance to CO_2: current knowledge and future prospects. Plant Cell Environ 31:602–621.

Flexas J, Barbour MM, Brendel O et al. (2012) Mesophyll diffusion conductance to CO_2: an unappreciated central player in photosynthesis. Plant Sci 193:70–84.

Galle A, Florez-Sarasa I, Aououad HE, Flexas J (2011) The Mediterranean evergreen *Quercus ilex* and the semi-deciduous *Cistus albidus* differ in their leaf gas exchange regulation and acclimation to repeated drought and re-watering cycles. J Exp Bot 62:5207–5216.

Galloway JN, Dentener FJ, Capone DG et al. (2004) Nitrogen cycles: past, present, and future. Biogeochemistry 70:153–226.

Galloway JN, Townsend AR, Erisman JW, Bekunda M, Cai ZC, Freney JR, Martinelli LA, Seitzinger SP, Sutton MA (2008) Transformation of the nitrogen cycle: recent trends, questions, and potential solutions. Science 320:889–892.

Genty B, Briantais JM, Baker NR (1989) The relationship between the quantum yield of photosynthetic electron-transport and quenching of chlorophyll fluorescence. Biochim Biophys Acta 990:87–92.

Gessler A, Rienks M, Rennenberg H (2000) NH_3 and NO_2 fluxes between beech trees and the atmosphere—correlation with climatic and physiological parameters. New Phytol 147:539–560.

Gessler A, Rienks M, Rennenberg H (2002) Stomatal uptake and cuticular adsorption contribute to dry deposition of NH_3 and NO_2 to needles of adult spruce (*Picea abies*) trees. New Phytol 156:179–194.

Grundmann GL, Lensi R, Chalamet A (1993) Delayed NH_3 and N_2O uptake by maize leaves. New Phytol 124:259–263.

Harley PC, Loreto F, Dimarco G, Sharkey TD (1992) Theoretical considerations when estimating the mesophyll conductance to CO_2 flux by analysis of the response of photosynthesis to CO_2. Plant Physiol 98:1429–1436.

Hassiotou F, Renton M, Ludwig M, Evans JR, Veneklaas EJ (2010) Photosynthesis at an extreme end of the leaf trait spectrum: how does it relate to high leaf dry mass per area and associated structural parameters? J Exp Bot 61:3015–3028.

Herrera M, Garvin JL (2011) Aquaporins as gas channels. Pflug Arch Eur J Phy 462:623–630.

Hove RM, Bhave M (2011) Plant aquaporins with non-aqua functions: deciphering the signature sequences. Plant Mol Biol 75:413–430.

Kaldenhoff R, Ribas-Carbo M, Flexas J, Lovisolo C, Heckwolf M, Uehlein N (2008) Aquaporins and plant water balance. Plant Cell Environ 31:658–666.

Kogami H, Hanba YT, Kibe T, Terashima I, Masuzawa T (2001) CO_2 transfer conductance, leaf structure and carbon isotope composition

of *Polygonum cuspidatum* leaves from low and high altitudes. Plant Cell Environ 24:529–537.
Krupa SV (2003) Effects of atmospheric ammonia (NH_3) on terrestrial vegetation: a review. Environ Pollut 124:179–221.
Kruse E, Uehlein N, Kaldenhoff R (2006) The aquaporins. Genome Biol 7: Art. no. 206.
Lanigan GJ, Betson N, Griffiths H, Seibt U (2008) Carbon isotope fractionation during photorespiration and carboxylation in *Senecio*. Plant Physiol 148:2013–2020.
Lichtenthaler HK (1987) Chlorophylls and carotenoids: pigments of photosynthetic biomembranes. In: Packer L, Douce R (eds) Methods in enzymology. Academic Press, New York, pp 350–382.
Loreto F, Harley PC, Dimarco G, Sharkey TD (1992) Estimation of mesophyll conductance to CO_2 flux by 3 different methods. Plant Physiol 98:1437–1443.
MacRobbie E (2006) Control of volume and turgor in stomatal guard cells. J Membrane Biol 210:131–142.
Massad RS, Tuzet A, Loubet B, Perrier A, Cellier P (2010) Model of stomatal ammonia compensation point (STAMP) in relation to the plant nitrogen and carbon metabolisms and environmental conditions. Ecol Model 221:479–494.
Maurel C, Verdoucq L, Luu DT, Santoni V (2008) Plant aquaporins: membrane channels with multiple integrated functions. Annu Rev Plant Biol 59:595–624.
McMurtrie RE, Wang YP (1993) Mathematical models of the photosynthetic response of tree stands to rising CO_2 concentrations and temperatures. Plant Cell Environ 16:1–13.
Musa-Aziz R, Chen LM, Pelletier MF, Boron WF (2009) Relative CO_2/NH_3 selectivities of AQP1, AQP4, AQP5, AmtB, and RhAG. Proc Natl Acad Sci USA 106:5406–5411.
Niinemets U, Cescatti A, Rodeghiero M, Tosens T (2005) Leaf internal diffusion conductance limits photosynthesis more strongly in older leaves of Mediterranean evergreen broad-leaved species. Plant Cell Environ 28:1552–1566.
Parry MAJ, Andralojc PJ, Scales JC, Salvucci ME, Carmo-Silva AE, Alonso H, Whitney SM (2013) Rubisco activity and regulation as targets for crop improvement. J Exp Bot 64:717–730.
Pinho P, Dias T, Cruz C, Sim Tang Y, Sutton MA, Martins-Loução M-A, Máguas C, Branquinho C (2011) Using lichen functional diversity to assess the effects of atmospheric ammonia in Mediterranean woodlands. J Appl Ecol 48:1107–1116.
Pinho P, Theobald MR, Dias T, Tang YS, Cruz C, Martins-Loução MA, Máguas C, Sutton M, Branquinho C (2012) Critical loads of nitrogen deposition and critical levels of atmospheric ammonia for semi-natural Mediterranean evergreen woodlands. Biogeosciences 9:1205–1215.
Pinto-Marijuan M, de Agazio M, Zacchini M, Santos MA, Torne JM, Fleck I (2007) Response of transglutaminase activity and bound putrescine to changes in light intensity under natural or controlled conditions in *Quercus ilex* leaves. Physiol Plantarum 131:159–169.
Polander BC, Barry BA (2012) A hydrogen-bonding network plays a catalytic role in photosynthetic oxygen evolution. Proc Natl Acad Sci USA 109:6112–6117.
Pompelli MF, Martins SC, Antunes WC, Chaves AR, DaMatta FM (2010) Photosynthesis and photoprotection in coffee leaves is affected by nitrogen and light availabilities in winter conditions. J Plant Physiol 167:1052–1060.
Poorter H, Niinemets U, Poorter L, Wright IJ, Villar R (2009) Causes and consequences of variation in leaf mass per area (LMA): a meta-analysis. N Phytologist 182:565–588.
Qiao Z, Murray F (1997) Effects of atmospheric nitrogen dioxide on uptake and assimilation of ammonium in Soybean plants. J Plant Nutr 20:1183–1190.
Rivas-Martínez S, Penas A, Díaz TE (eds) (2004) Bioclimatic map of Europe. Bioclimates: Cartographic Service. University of León, Spain.
Rockstrom J, Steffen W, Noone K et al. (2009) A safe operating space for humanity. Nature 461:472–475.
Rodrigues C, Brunner M, Steiman S, Bowen GJ, Nogueira JMF, Gautz L, Prohaska T, Máguas C (2011) Isotopes as tracers of the Hawaiian coffee-producing regions. J Agric Food Chem 59:10239–10246.
Sandusky PO, Yocum CF (1984) The chloride requirement for photosynthetic oxygen evolution—analysis of the effects of chloride and other anions on amine inhibition of the oxygen-evolving complex. Biochim Biophys Acta 766:603–611.
Sparks JP (2009) Ecological ramifications of the direct foliar uptake of nitrogen. Oecologia 159:1–13.
Sutton MA, Burkhardt JK, Guerin D, Nemitz E, Fowler D (1998) Development of resistance models to describe measurements of bi-directional ammonia surface-atmosphere exchange. Atmospheric Environ 32:473–480.
Sutton MA, Howard C, Erisman JW, Billen G, Bleeker A, Grennfelt P, van Grinsven H, Grizzetti B (eds) (2011) The European nitrogen assessment. Cambridge University Press, Cambridge, UK, 664 pp.
Tang YS, Cape JN, Sutton MA (2001) Development and types of passive samplers for monitoring atmospheric NO_2 and NH_3 concentrations. Sci World J 1:513–529.
Tholen D, Zhu X-G (2011) The mechanistic basis of internal conductance: a theoretical analysis of mesophyll cell photosynthesis and CO_2 diffusion. Plant Physiol 156:90–105.
Tosens T, Niinemets U, Vislap V, Eichelmann H, Castro Diez P (2012*a*) Developmental changes in mesophyll diffusion conductance and photosynthetic capacity under different light and water availabilities in *Populus tremula*: how structure constrains function. Plant Cell Environ 35:839–856.
Tosens T, Niinemets U, Westoby M, Wright IJ (2012*b*) Anatomical basis of variation in mesophyll resistance in eastern Australian sclerophylls: news of a long and winding path. J Exp Bot 63:5105–5119.
Tyerman SD, Niemietz CM, Bramley H (2002) Plant aquaporins: multifunctional water and solute channels with expanding roles. Plant Cell Environ 25:173–194.
Uehlein N, Otto B, Hanson DT, Fischer M, McDowell N, Kaldenhoff R (2008) Function of *Nicotiana tabacum* aquaporins as chloroplast gas pores challenges the concept of membrane CO_2 permeability. Plant Cell 20:648–657.
Uehlein N, Sperling H, Heckwolf M, Kaldenhoff R (2012) The *Arabidopsis* aquaporin PIP1;2 rules cellular CO_2 uptake. Plant Cell Environ 35:1077–1083.
Villar R, Held AA, Merino J (1995) Dark leaf respiration in light and darkness of an evergreen and a deciduous plant-species. Plant Physiol 107:421–427.
Werner C, Unger S, Pereira JS, Maia R, David TS, Kurz-Besson C, David JS, Maguas C (2006) Importance of short-term dynamics in carbon isotope ratios of ecosystem respiration ($\delta^{13}C_R$) in a Mediterranean oak woodland and linkage to environmental factors. N Phytol 172:330–346.
Winter K, Usuda H, Tsuzuki M, Schmitt M, Edwards GE, Thomas RJ, Evert RF (1982) Influence of nitrate and ammonia on photosynthetic characteristics and leaf anatomy of *Moricandia arvensis*. Plant Physiol 70:616–625.
Wudick MM, Luu DT, Maurel C (2009) A look inside: localization patterns and functions of intracellular plant aquaporins. New Phytol 184:289–302.
Zhu XY, Chen GC, Zhang CL (2001) Photosynthetic electron transport, photophosphorylation, and antioxidants in two ecotypes of reed (*Phragmites communis* Trin.) from different habitats. Photosynthetica 39:183–189.